A Study of Electric-Field Breakdown in *E*-Plane Lines at Centimeter and Millimeter Wavelengths

MICHEL M. NEY, MEMBER, IEEE, SREE R. VALLURI, WARREN YUE, STUDENT MEMBER, IEEE, GEORGE I. COSTACHE, SENIOR MEMBER, IEEE, AND WOLFGANG J. R. HOEFER, SENIOR MEMBER, IEEE

Abstract—**The microwave field breakdown in various *E*-plane transmission lines is investigated theoretically in the frequency range from 1 to 140 GHz. The influence of frequency, pressure, temperature, and inhomogeneity of the applied field on the breakdown field value is discussed. The peak power-handling capability of unilateral and bilateral finlines is determined theoretically using a quasi-static evaluation of the field distribution. It is found that finlines, even with small gap widths, can handle pulse power levels well above the capability of present solid-state devices. Preliminary breakdown measurements in *X*-band have confirmed the validity of the theoretical predictions.**

I. Introduction

RENEWED INTEREST in the millimeter-wave range has focused the attention of many researchers on planar transmission media such as *E*-plane structures. Most efforts have been directed toward the determination of the propagation constant and characteristic impedance. However, no data on the power-handling capability of such lines have been reported in the literature. Yet, this aspect is becoming increasingly important since higher and higher power levels become available from solid-state devices. Given the trend toward complete integration of receiver/transmitter systems in planar technology, there is a growing concern about the power that *E*-plane structures can handle. The present study has been undertaken to address this concern.

So far, most theoretical as well as experimental work on power-handling capability has been restricted to air-filled waveguide structures. Pioneering work was carried out by Hopfer [1] on the peak power-handling capability of ridged waveguides. The innovation in this work resided in the use of rounded ridge profiles. Hopfer used a static approach to determine the electric field in the gap region, and introduced correction factors to compute the maximum power under dynamic conditions. Jablonsky [2] computed the maximum power that can be transmitted in a dielectric rod waveguide, accounting for both electrical breakdown and dielectric dissipation. The interesting conclusion was that, in continuous wave (CW) operation, the dielectric waveguide would melt before breakdown occurred. This observation is also true in the case of *E*-plane structures, where the continuous power capability is always much lower than the peak power rating.

The present paper concentrates on the latter aspect of the power limitation, namely, the field breakdown phenomenon. This is the limiting factor in pulsed signal operation, which is typical in radar systems for ranging and tracking applications. The maximum power is thus determined by the maximum field strength that can exist in the structure. Indeed, for narrow pulse signals, one can legitimately assume that, by virtue of the relatively low average power involved in this case, dissipation in the dielectric substrate and in the conducting strips is low and that breakdown in the air or in the dielectric will occur before the temperature in the structure rises significantly, even at high frequencies, where dielectric losses and dissipation in the conductors are increased.

Finally, although much work has been reported on breakdown phenomena, especially at low pressure [3]–[5], almost no data are available in the millimeter-wave range. In addition, the field configuration in *E*-plane structures is highly inhomogeneous, and dc electric fields (biasing fields) may be superimposed on the dynamic fields when solid-state devices are mounted across the slot. Also, relatively strong dc magnetic fields exist in nonreciprocal devices such as circulators and isolators [6]. Thus, along with parameters such as frequency, temperature, pressure, and pulsed signal duration, the above factors influence the ionization process which leads to breakdown. A thorough investigation of the breakdown mechanism is presented in this paper. It allows the designer to extrapolate the breakdown value of the electric field in various practical situations and then to evaluate the peak power-handling capability of a given *E*-plane transmission line.

II. Theory

A. Power Calculation

Fig. 1 shows the geometry of typical *E*-plane lines, in this case a finline. The peak power-handling capability of such a structure is determined by the maximum field

Manuscript received August 18, 1986; revised December 15, 1986. This work was supported in part by the Natural Science and Engineering Research Council of Canada.

M. M. Ney, W. Yue, G. I. Costache, and W. J. R. Hoefer are with the Department of Electrical Engineering, University of Ottawa, Canada K1N 6N5.

S. R. Valluri is with the Department of Applied Mathematics, University of Western Ontario, London, Canada N6A 5B9.

IEEE Log Number 8613466.

0018-9480/87/0500-0502$01.00 ©1987 IEEE

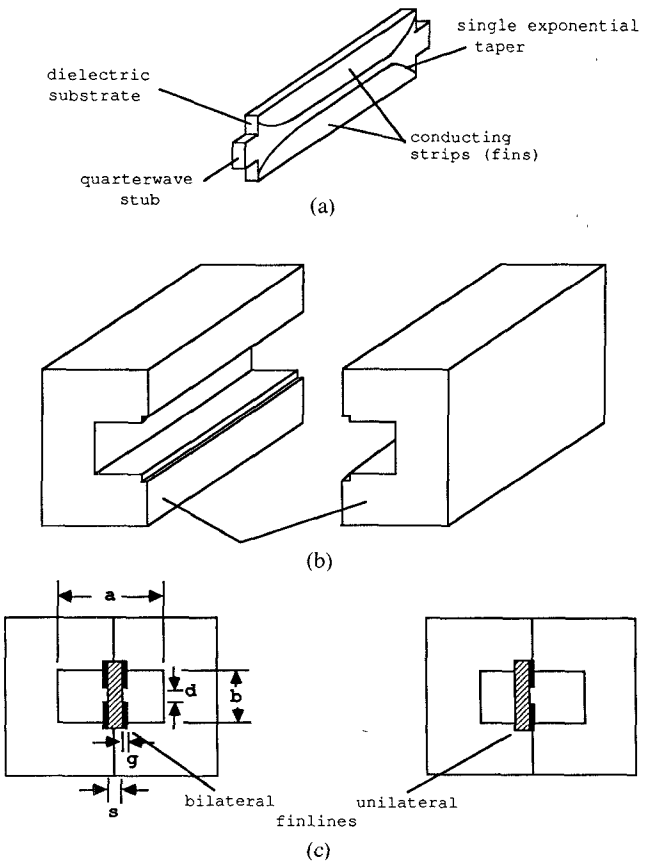

Fig. 1. Geometry of a typical *E*-plane line (finline). (a) Finline insert with two exponential transitions to waveguide. (b) Finline housing with inner standard waveguide dimensions. (c) Cross section of bilateral and unilateral finlines.

strength in the gap between the fins. Consequently, the computation of the peak power capability must start with the determination of the field distribution and the maximum field strength, which, for obvious reasons, occurs in the vicinity of the conductor edges.

Many techniques have been proposed to compute the electromagnetic field of inhomogeneous transmission lines. The most prominent among them are the spectral-domain (SD) [7], the transmission line matrix (TLM) [8], and the finite-element (FE) [9] method. In order to avoid singularities in the field strength on the conductor edges, structures with realistic conducting strip profiles, such as those shown in Fig. 2, must be considered. The most suitable technique that can handle these types of profiles are the FE and TLM methods.

Since the *E*-plane lines are inhomogeneous structures, they propagate hybrid modes (a combination of TE and TM modes). In this case, the problem is three-dimensional and the above techniques are difficult to implement. But since the dominant mode is almost a TE mode, a quasi-static approach can be used which makes the problem two-dimensional. To this end, the electric field between the fins is identical to the one of the structure illustrated in Fig. 3.

The electromagnetic field in the gap between the conductors can thus be found approximately with the 2-D

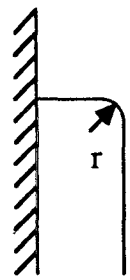

Fig. 2. Edge profile used for numerical computations.

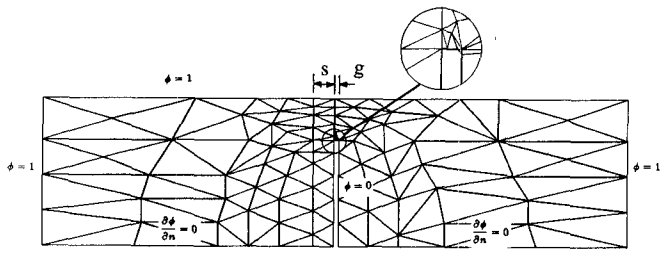

Fig. 3. Triangle decomposition for a finite-element-method solution.

finite-element method, which is very convenient for complicated geometries, such as in Fig. 3. It is noteworthy that although the paper treats only the case of finline structures, the assertion of a quasi-static field in the region of interest applies to many other cases, such as *E*-plane lines without dielectric (e.g., ridged waveguides), coplanar waveguides, slotlines, and coplanar striplines. Thus, the procedure described below holds for a wide variety of structures.

The method to determine the maximum power that can be transmitted in a given structure can be summarized as follows.

i) Find the maximum field strength in a given structure, using an appropriate method. Make the problem two-dimensional if possible.

ii) Set the maximum field strength equal to the appropriate breakdown value, accounting for all parameters such as frequency, pressure, and temperature, and geometry.

iii) Find the corresponding voltage between the conductors.

iv) Compute the corresponding transmitted power using the following relation:

$$P_{\max} = \frac{V_{\max}^2}{2Z_0} \tag{1}$$

where Z_0 is the voltage–power impedance of the line, and $V_{\max}$ the voltage computed under iii).

It is important to mention that the computation of the characteristic impedance cannot be done using the quasi-static approach. Indeed, the amount of power in a transmission line which does not propagate a pure transverse electromagnetic (TEM) mode depends on the frequency. Thus, the hybrid character of the electromagnetic wave field propagating in the structure must be accounted for. In this paper, a highly efficient program using the SD technique [10] was used to determine the characteristic

impedance of finline structures. For the purpose of this study, the effect of finite metallization thickness on Z_0 has been neglected, since it modifies the characteristic impedance by a few percent only [11], except for extremely narrow gaps. The dominant factor, in any case, is the variation of Z_0 with frequency.

B. Finite-Element Formulation

As mentioned before, of the methods available for computing an electrostatic field, the finite-element method is particularly effective because of its ability to handle complicated geometries such as those considered in this paper. In addition, it has a proven accuracy in electrostatic problem solutions. This feature is very important when we consider the sharp edges of the conducting strips, which are the regions of interest in our case.

The electrostatic problem to be solved in this case is described by the following equation [12]:

$$\nabla\cdot(\epsilon\nabla\phi)=0 \tag{2}$$

with associated Neumann and Dirichlet boundary conditions. The problem is to find the electrostatic potential for an inhomogeneous region, where the permittivity is a function of position, from which the corresponding electric field can be easily derived.

For our field problem, the Neumann boundary conditions are homogeneous, and the Dirichlet boundary conditions are inhomogeneous (see, for instance, Fig. 3). In this situation, the appropriate functional to be minimized is given by [12]

$$F(\phi)=\int\int_S \epsilon(\nabla\phi)^2\,dx\,dy \tag{3}$$

for which the Neumann boundary conditions are natural. For this reason, the trial functions used for minimization of the functional should satisfy only the Dirichlet boundary conditions. The functional (3), which is proportional to the energy of the system, has (2) as its Euler–Lagrange equation, and its solution can be obtained by minimization of (3).

The region where the field distribution was established is divided into triangles as shown in Fig. 3. The trial function for each triangle used for this application is linear and is given by [12]:

$$\phi=\sum_{n=i,j,k}\alpha_n(x,y)\phi_n \tag{4}$$

where

$$\alpha_i(x,y)=\left[(x_jy_k-x_ky_j)+(y_j-y_k)x+(x_k-x_j)y\right]\Big/\text{twice the area of the triangle.}$$

Here, the circular permutation of the subscripts in the sequence i, j, k, represents the shape functions used in each triangle. The node potentials ϕ are used as variational parameters, and after the minimization of the functional (3), one ends up with a linear system of equations of the form

$$[S][\phi]=[T] \tag{5}$$

where $[S]$ is a symmetrical matrix by virtue of the self-adjointness of the operator in (2), and $[\phi]$ and $[T]$ are column vectors which contain the unknown node potentials and the information about the Dirichlet values on the boundary, respectively.

III. Theoretical Study of the Breakdown Field in Slot-Type Structures

The electrical breakdown of a gas is the transition from an insulating to an almost completely conducting state. The early pioneering work of Townsend [3] defined a criterion that allows a quantitative description of breakdown. It was originally intended for direct-current discharges but has been useful as well for ac discharges at any frequency, including microwave and millimeter-wave regions. Herlin and Brown [13] clearly demonstrated the relevance of the Townsend criterion to microwave breakdown as far as basic processes in high-frequency discharges are concerned.

During a gas discharge, electrons that are being produced by ionization can be removed by several loss processes, such as recombinations with ions, diffusion, and attachment. In the case described in this paper, the diffusion and loss in the conductors are the dominant factors. Suppose an unbounded volume in which there exists a certain concentration n of electrons. The diffusion and loss processes are governed by the following equation [5]:

$$\frac{\partial n}{\partial t}=\nabla^2(Dn)+n\nu_i \tag{6}$$

where D is the diffusion rate and ν_i the ionization rate per electron. The above equation can be solved by the technique of separation of variables:

$$\frac{dn}{dt}=(\nu_i-\gamma)n \tag{7}$$

$$\nabla^2 n=-\frac{\gamma n}{D} \tag{8}$$

where γ is a constant to be determined.

If ν_i is independent of time, the solution for (7) is easily found:

$$n=n_0\exp\{(\nu_i-\gamma)t\} \tag{9}$$

where γ depends on the diffusion coefficient and the geometry of the problem. When an increasing electric field is applied to a medium where a small number of free electrons are present, their concentration grows until the field has reached a value at which the energy imparted to the electrons is sufficiently high to produce secondary electrons by collision. Hence, the production rate increases rapidly and can exceed the loss rate. Thus, since very large numbers are involved in the exponent of (9), the concentration of free electrons can become extremely large in a relatively short period of time, even though the production rate is only infinitesimally larger than the loss rate. The Townsend criterion is defined as saying that breakdown occurs when the ionization rate equals the loss rate.

For sufficiently high frequencies, the motion of the electron cloud is periodically reversed; hence, the loss of free electrons into the conducting boundaries cannot take place. Consequently, breakdown can occur at lower field values, depending on the distance between the conducting boundaries.

A. Diffusion Length

The geometry of the volume in which the ionization process takes place is an important factor, one that can be characterized by the diffusion length concept. In regard to this work, we shall consider the geometry illustrated in Fig. 4 for the case of a finline structure. Since the field is highly concentrated between the fins where the breakdown most likely occurs, we shall make the approximation that it is uniform in the gap, which implies an upper bound for the breakdown field value, and decreases rapidly outside. Consequently, the ionization rate is independent of the location and (8) can be solved in rectangular coordinates:

$$n = n_0 \cos\frac{\pi x}{d}\cos\frac{\pi y}{2g} \tag{10}$$

where it is assumed that the concentration is zero on the surface of the conductors, maximum on the dielectric wall, and negligible outside the gap. Substituting (10) into (8) yields the eigenvalues, defined by

$$\left(\frac{\pi}{d}\right)^2+\left(\frac{\pi}{2g}\right)^2=\frac{\gamma}{D}=\frac{1}{\Lambda^2} \tag{11}$$

where the relevant geometrical parameters are illustrated in Fig. 4, and Λ is the diffusion length. The length Z is theoretically infinite. However, experiments have confirmed that breakdown does not occur simultaneously along the whole structure, due to the irregularities of the gap width. Therefore, the diffusion length must be modified as follows:

$$\frac{1}{\Lambda^2}=\left(\frac{\pi}{d}\right)^2+\left(\frac{\pi}{2g}\right)^2+\left(\frac{\pi}{Z}\right)^2 \tag{12}$$

where Z is the longitudinal distance over which breakdown occurs. Note that in the absence of a dielectric, n must be maximum at the center and zero at the limits of the gap region. In this case, (10)–(12) must be modified accordingly.

B. Influence of Frequency and Effective Field Concept

At high frequencies and with sufficiently large amplitude of the electric field, the electrons can be swept completely across the gap and collide with the conducting walls during a half cycle. This is the case in finlines of realistic characteristic impedance, where the conducting fins are relatively close to each other. For an electric field of the form

$$E = E_p \sin\omega t \tag{13}$$

where $\omega = 2\pi f$ is the angular frequency, one has the following relation for the breakdown field E_B in the oscillation amplitude limit [5]:

$$E_B = 2\pi\cdot 10^5\cdot\frac{p}{\lambda}\cdot\Lambda \tag{14}$$

where p is the pressure and $\lambda = c/f$ the wavelength. Equation (14) suggests a linear relation between E_B and the frequency f. Breakdown values in the X-band, for example, can be calculated at given p and f by this formula. It certainly would be tempting to extrapolate (14) to higher field frequencies beyond the X-band. Such a procedure would only give an extremely crude indication of E_B for higher frequencies. Indeed, the transfer of energy from the electric field to the electrons becomes less efficient as the frequency increases. The inertia of the electrons results in an out-of-phase component. The energy transfer efficiency may be expressed through an effective field E_e [14], which takes into account the collision frequency ν_{eff}:

$$E_e = E\Big/\sqrt{2\left(1+\frac{\omega^2}{\nu_{\text{eff}}^2}\right)}\,. \tag{15}$$

A theoretical analysis making use of the effective field concept has correlated all the breakdown data for air. The form of the correlation is such that it makes possible accurate predictions of breakdown fields for both CW and pulsed conditions over a wide range of the experimental variables [5]. It is also reasonable to make meaningful extrapolations to neighboring physical regions for which experimental data are not available. The predictions are claimed with reasonable certainty for frequencies up to 100 GHz over pressure ranges corresponding to an altitude variation from ground level to about 100 km [5]. With the use of the effective field concept, predictions can be extended up to 140 GHz. Following Lupan [15], the following relation can be used, for example, for frequencies above 25 GHz:

$$\frac{\nu_i}{p} = 2.5\cdot 10^7\left\{1.45(E_e/p)^{1/2}+0.01(E_e/p)^{3/2}\right\}\cdot\exp\left(\frac{-278}{E_e/p}\right)\ \text{s}^{-1}\ \text{torr}^{-1} \tag{16}$$

where ν_i is the average ionization rate of the heavy particles in air, E_e is the effective field, and p is the pressure. The amplitude of the microwave electric field E can then

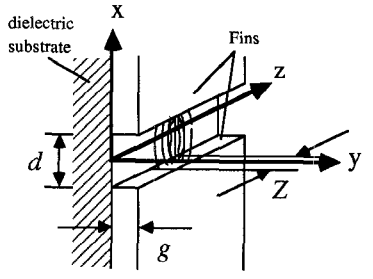

Fig. 4. Geometry pertaining to the evaluation of the diffusion length for a finline structure.

be calculated using (15), where the effective electron collision frequency is $\nu_{\text{eff}} = 5.3\times10^9 p$ [Hz]. For instance, Fig. 5 shows the electric-field breakdown values as a function of the frequency for atmospheric pressure ($p = 760$ mm) and for ionization rates in the range $10^7 < \nu_i < 9\times10^9$ Hz. As the frequency increases beyond the X-band region, the breakdown field value does not increase indefinitely, but saturates to a value which depends on the ionization rate. In the X-band region, the oscillation amplitude limit depends on the geometry through the parameter Λ. The lower limit corresponds to the realistic case where, due to the irregularities of the gap width, the breakdown occurs only over a region as small as the irregularities. On the other hand, the upper limit indicates the ideal case of a breakdown occurring over an infinitely long line. It is noteworthy that around 10 GHz both the oscillation amplitude limit and the effective field concepts are applicable. This provides the possibility of obtaining the correct ionization rate from the intersection between the curves pertaining to both methods (see Fig. 5).

Measurements of pulsed breakdown fields are subject to more uncertainty because the shape, length of pulse, and repetition rate all have a bearing on the result. The pulsed breakdown fields are about 10-percent higher than CW operation for typical applications at most microwave frequencies. Other factors may also influence the field breakdown value. For instance, the evaluation of the breakdown value here does not account for the heat that is produced in the conducting strips and the dielectric substrate. This is because of the relatively low average power produced by pulsed signals (typically 10^{-3}-duty cycle) for radar operation. However, for higher average power levels, substantial increases of the ambient and component temperature will lower the breakdown value, especially in the presence of loose particles [4]. Moreover, above a certain level, heat dissipations may be the limiting factor. Finally, it is supposed that the environment is clean of dust and loose particles.

C. Superimposed DC and AC Fields

The superposition of dc and ac electric fields arises when biasing of solid-state devices is needed. Ionization triggering can be made more difficult by the superimposition of a dc electric field. The modified diffusion length Λ_{dc} for superimposed fields is [5]

$$\frac{1}{\Lambda_{\text{dc}}^2} = \frac{1}{\Lambda^2} + \left(\frac{\mu E_{\text{dc}}}{2D}\right)^2 \tag{17}$$

and

$$\frac{\nu_i}{D} = \frac{1}{\Lambda_{\text{dc}}^2} \tag{18}$$

is the new breakdown condition. In (17), μ is the mobility, D is the diffusion coefficient, and E_{dc} is the applied dc electric field; Λ_{dc} is computed from (11). The factor D/μ can be calculated from the average electron energy u_{ave}:

$$\frac{D}{\mu} = \frac{2}{3}\cdot u_{\text{ave}} = \frac{1}{3}\frac{m\nu^2}{e} \tag{19}$$

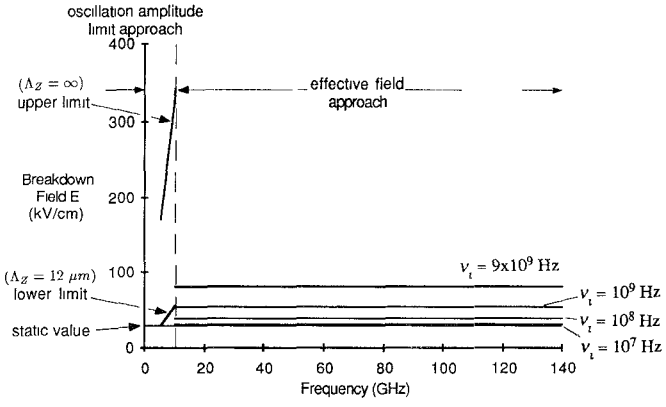

Fig. 5. Breakdown field values in the air versus frequency (theoretical prediction). Pressure $p = 760$ mmHg. ν_i = ionization rate. The curves in the oscillation amplitude limit approach have been evaluated in the configuration given in Fig 4. The curves in the effective field approach range have been obtained from [15].

for a Maxwellian velocity distribution [5]. Once Λ_{dc} is determined, the corresponding breakdown value is calculated from (14), where Λ is replaced by Λ_{dc}.

D. Combination of DC Magnetic and AC Electric Fields

For ferrite devices, a dc magnetic field is superimposed on a high-frequency ac electric field. A static magnetic field perpendicular to the ac electric field will cause a general increase of the value of the breakdown field. However, the general shape of the breakdown field frequency characteristic (given by (16)) is not changed [17]. In situations in which the magnetic field is uniform and in one direction, for example, along the longitudinal direction, say the z axis, the diffusion length becomes, in Cartesian coordinates [18],

$$\frac{1}{\Lambda_b^2} = \left(\frac{1}{\Lambda_X^2} + \frac{1}{\Lambda_Y^2}\right)\cdot\frac{1}{1+b^2} + \frac{1}{\Lambda_Z^2} \tag{20}$$

where B is the magnetic field magnitude and

$$b^2 = \frac{\omega_b^2}{\nu_{\text{eff}}^2} = \frac{e^2B^2}{m^2\nu_{\text{eff}}^2}. \tag{21}$$

The effect of the magnetic field is equivalent to enlarging the size of the breakdown region by the factor $\sqrt{1+\omega_b^2/\nu_{\text{eff}}^2}$ in the directions perpendicular to the magnetic field. An increase in the breakdown field value is also possible due to the effective rise of pressure when a magnetic field is superimposed on a low-frequency electric field. Once Λ is computed, the breakdown value of the field is computed with (14), where Λ is replaced by Λ_b. However, for appreciable values of the magnetic field, which imply a relatively great Lorentz force, one has to study carefully an expansion of the Boltzmann transport equation in spherical harmonics in space and in Fourier series in time. The resulting differential equation for the distribution function can be integrated to determine electrical breakdown values [18].

TABLE I
DIMENSIONS OF THE FINLINE STRUCTURES

	a(mm)	b(mm)	s(μm)	g(μm)
WR-28	7.112	3.556	254	17
WR-90	22.86	10.16	762	34

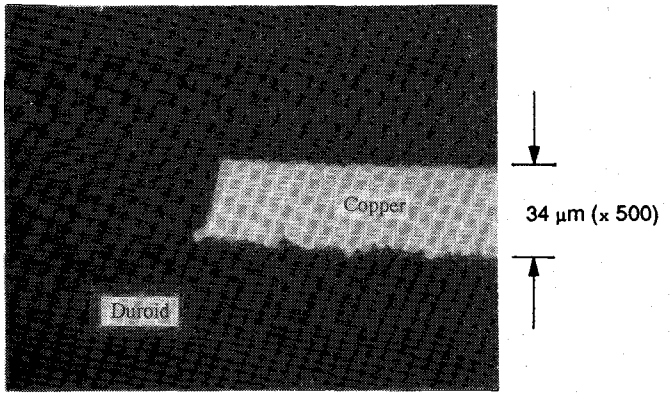

Fig. 6. Optical micrograph of a sectioned finline structure (Courtesy of J. Noad, Communications Research Center, Ottawa, Canada).

IV. THEORETICAL RESULTS

The theoretical breakdown field values were computed for two unilateral and two bilateral finlines with dimensions given in Table I. The equivalent structures used for the computation of the potential distribution with the FEM are shown in Fig. 4. The geometry of the conductor profiles is revealed by micrography of a sectioned finline, shown in Fig. 6. The assumption of right-angle corners is a crude approximation, and rounded corners, such as those shown by Fig. 2, were used. It is noteworthy that the finite-element method is indeed suitable for these types of complicated geometry.

Two frequency bands were considered, namely, *X*- and *Ka*-bands, for which the corresponding waveguide enclosures were WR-90 and WR-28, respectively. Table II shows the maximum field strength values computed for different gap widths across which 1 V is applied. As expected, the maximum field strength increases when the gap width decreases. Another observation is that the values do not vary significantly when the structures used in both bands are compared. This is easily explained by the fact that since the field is confined in the gap, the dimensions of the enclosures have very little influence.

As mentioned before, although a static approach is used for field computations, the corresponding power transmitted by the line is frequency dependent and should be evaluated using dynamic approaches. The impedance of the lines was evaluated with the spectral-domain method. For reasons stated before, the assumption of infinitely thin conductors can be made for this computation. The corresponding maximum transmitted power, computed from (1), is plotted in Fig. 7(a) and (b) for unilateral and bilateral structures, respectively, in *Ka*-band. The irregular behavior of the line corresponding to $d = 1.5$ mm is due to the peculiar frequency characteristic of the power–voltage

TABLE II
COMPARISON OF THE MAXIMUM PEAK POWER-HANDLING CAPACITY OF FINLINES WITH CORRESPONDING WAVEGUIDE STRUCTURES

Maximun power(kW)	Finline unilateral	Finline bilateral	Empty waveguide
WR-28	2.3	3.0	128.2
WR-90	4.5	4.5	1160.

Gap width = 1 mm. Finline dimensions as in Table I ($\epsilon_r = 2.22$).

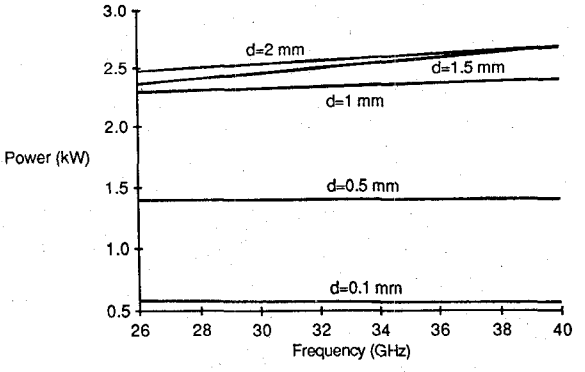

(a)

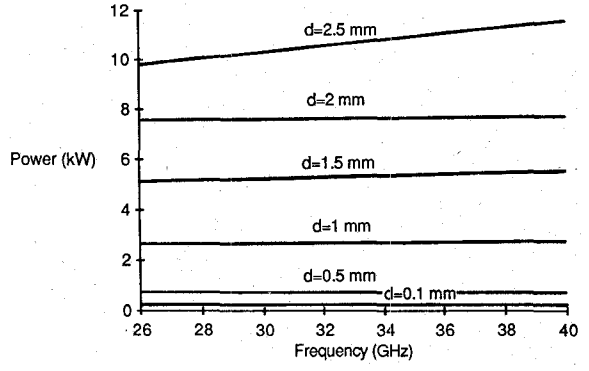

(b)

Fig. 7. Peak power-handling capability of WR-28 (a) unilateral and (b) bilateral finline structures for different gap widths evaluated with the FEM; $g = 17\ \mu$m, $s = 254\ \mu$m, and $\epsilon_r = 2.22$.

impedance of the finline described in detail by Schmidt and Itoh [7]. For convenience, the values of the characteristic impedance of the corresponding finlines are shown in Fig. 8(a) and (b) as a function of the gap width for different frequencies. Diagrams of Fig. 8 were established by assuming a static breakdown field value of 30 kV/cm in the air at atmospheric pressure. Corrections due to the geometry and the frequency can be made by using the diagram shown in Fig. 5. For instance, for an ionization rate of 10^9 Hz, the maximum admissible field value would be multiplied by 1.8 and, consequently, the power would be increased by a factor of 3.4. For the upper *X*-band region, since it is at the limit of both approaches, the correction factor can be evaluated by the effective field approach or, if ν_i is not known, by the oscillation amplitude limit.

Table II shows the maximum transmissible peak power of finline structures ($d = 1$ mm) compared with the corre-

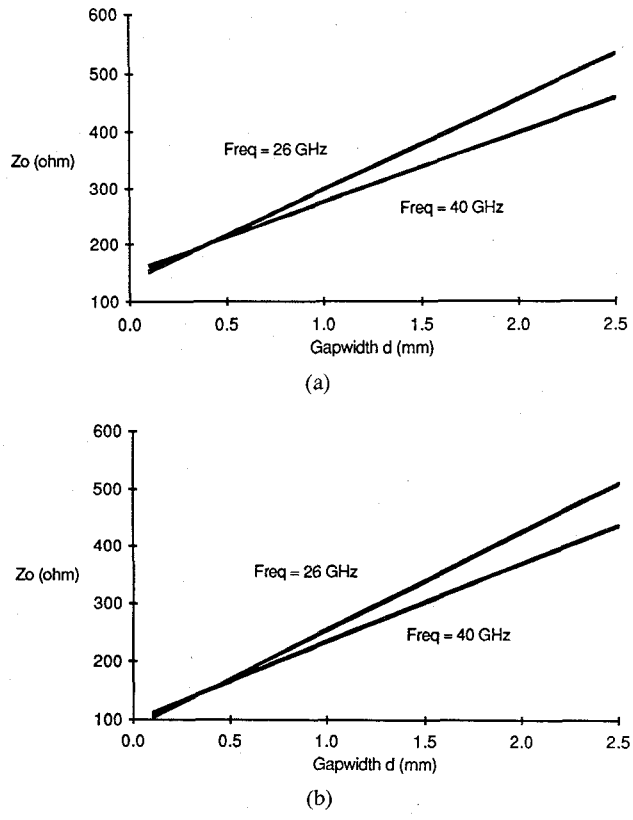

Fig. 8. Impedance versus gap width for WR-28 (a) unilateral and (b) bilateral finline structures evaluated by the SDM; $g = 17\ \mu$m, $s = 254\ \mu$m, $\epsilon_r = 2.22$.

sponding empty-waveguide structure (maximum value in the band). The theoretical predictions indicate that, as expected, the peak power-handling capability of an empty waveguide is severely affected by the introduction of the planar insert.

Experimental procedures were carried out to verify the validity of the approach presented in this paper, and results will be presented in a future communication. However, if one considers the case of finlines used with solid-state device generators, their peak power-handling capability is still one or two orders of magnitude above the peak power that those devices can generate.

V. Conclusions

A quasi-static approach to determine the maximum electric strength in *E*-plane planar structures has been proposed. The maximum peak power-handling capability of these lines has then been determined, and results for various finline structures have been presented.

A complete study of the breakdown mechanism in various finline configurations has been carried out. The value of the breakdown field is affected by the frequency and the geometry such that it is higher than the standard value of 30 kV/cm (in air), which is usually adopted in practice. On the other hand, a saturation occurs at very high frequencies when the collision frequency exceeds the field frequency.

Finally, it has been found that the peak power-handling capability of finline structures is more than two orders of magnitude below that of the commensurate empty waveguide. Nevertheless, if one considers the compatibility of finlines with solid-state devices, the peak power values that can be generated at the present state of the art are still one or two orders of magnitude below the peak power-handling capability of these lines.

Acknowledgment

The authors wish to thank J. Noad, Communication Research Center in Ottawa, for providing the micrographs of the finline profiles.

References

[1] S, Hopfer, "The design of ridged waveguides," *IRE Trans. Microwave Theory Tech.*, vol. MTT-31, pp. 20–29, Oct. 1955.
[2] D. G. Jablonski, "Power-handling capabilities of circular dielectric waveguide at millimeter wavelengths," *IEEE Trans. Microwave Theory Tech.*, vol. MTT-33, pp. 85–89, Feb. 1985.
[3] J. S. Townsend, *The Theory of Ionisation of Gases by Collision*. London: Constable, 1910.
[4] A. S. Acampora and P. T. Sproul, "Waveguide breakdown effects at high average power and long pulse length," *Bell Syst. Tech. J.*, vol. 51, no. 9, pp. 2065–2091, Nov. 1972.
[5] A. D. MacDonald, *Microwave Breakdown in Gases*. New York: Wiley, 1966.
[6] *Millimeter-Wave Ferrite and Waveguide Components*. Hughes Aircraft Company, Electron Dynamic Division, Torrance, CA, 1982.
[7] L.-P. Schmidt and T. Itoh, "Spectral-domain analysis of dominant and higher order modes in fin-lines," *IEEE Trans. Microwave Theory Tech.*, vol. MTT-28, pp. 981–985, Sept. 1980.
[8] P. B. Jones, "Application of transmission line matrix method to homogeneous waveguides of arbitrary cross-section," *Proc. IEEE*, vol. 119, Aug. 1972.
[9] B. H. McDonald, M. Friedman, and A. Wexler, "Variational solution of integral equations," *IEEE Trans. Microwave Theory Tech.*, vol. MTT-22, pp. 237–248, Mar. 1974.
[10] W. J. R. Hoefer, "Accelerated spectral domain analysis of *E*-plane circuits suitable for computer-aided design," in *URSI Int. Symp. Electromagnetic Theory Dig.* (Budapest, Hungary), Aug. 25–29, 1986.
[11] R. Vahldieck, "Accurate hybrid-mode analysis of various finline configurations including multilayered dielectrics, finite metallization thickness, and substrate holding grooves," *IEEE Trans. Microwave Theory Tech.*, vol. MTT-32, pp. 1454–1460, Nov. 1984.
[12] G. I. Costache, M. Slanina, and E. Della-Giacomo, "Finite element method used to some axisymmetrical insulation problems," *Rev. Roum. Sci. Techn., Ser. Electrotech. Energ.*, vol. 20, no. 4, pp. 475–481, 1975.
[13] M. R. Herlin and S. C. Brown, *Phys. Rev.*, vol. 74, pp. 291, 910, 1948.
[14] H. Margenau, *Phys. Rev.*, vol. 60, pp. 508, 1946.
[15] Y. A. Lupan, A. A. Krasutskii, and S. V. Zakrevskii, "Microwave breakdown field in air," *Sov. Phys.–Tech. Phys.*, vol. 23, no. 6, pp. 649–650, June 1978.
[16] A. D. MacDonald, D. U. Gaskell, and H. N. Gitterman, *Phys. Rev.*, vol. 130, pp. 1841, 1963.
[17] F. Kossel and K. Kreds, *Z. Phys. Rev.*, vol. 139, pp. 189, 154.
[18] B. Lax, W. P. Allis, and S. C. Brown, *J. Appl. Phys.*, vol. 21, pp. 1297, 1950.

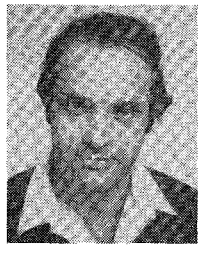

Michel M. Ney (S'83–M'83) received the engineer degree from the Swiss Federal Institute of Technology of Lausanne, Switzerland, in 1976 and the M.Sc. degree in electrical engineering from the University of Manitoba, Canada, in 1978.

During 1978 and 1979, he was with the Laboratory of Electromagnetism and Acoustics at the Swiss Federal Institute of Lausanne as a Research Associate. He joined the University of Ottawa, Canada, in 1979, where he completed

the Ph.D. degree in 1983. Since that time, he has been with the Department of Electrical Engineering of the University of Ottawa as an Assistant Professor. His main research interests are electromagnetic engineering and numerical methods.

Dr. Ney is a registered Professional Engineer in the province of Ontario, Canada.

✠

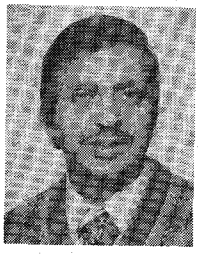

Sree Ram Valluri was born in Madras, India, on June 10, 1948. He received the. M.Sc. degree in physics from the India Institute of Technology, Kanpur, in 1968 and the M.Sc. in theoretical nuclear physics from the University of Ottawa, Ottawa, Canada in 1970. He obtained the Ph.D. from the University of Regina, Saskatchewan, Canada in May 1975 in high-energy relativistic astrophysics (photoproduction of gravitons in static electromagnetic fields and astrophysical applications).

From September 1975 to August 1978, he was a Research Associate and Special Lecturer at Regina, where he continued his work on gravitons with his thesis supervisor, Prof. G. Papini, and also worked in high-energy physics with Prof. D. Y. Kim. In 1979, he moved to the Georgia Institute of Technology, Atlanta, as a Research Associate with Prof. D. Finkelstein and worked on problems in quantum electrodynamics. He worked at the Institute of Theoretical Physics at the Justus Liebig University, Giessen, from October 1982 to August 1985 on problems at the borderline of atomic and nuclear physics. He also taught part-time for the University of Maryland/European Division from August 1984 to July 1985. Dr. Valluri is currently an Assistant Professor at the Department of Applied Mathematics, University of Western Ontario, Canada.

✠

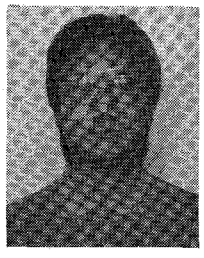

Warren Yue (S'84) was born in Hong Kong on Dec. 9, 1959. He received the B.A.Sc. and M.A.Sc. degrees in 1984 and 1986, respectively, from the University of Ottawa, Ottawa, Ontario, Canada. He has been engaged in research on planar transmission media and numerical technique, and is currently working toward the Ph.D. degree in electrical engineering at the University of Ottawa.

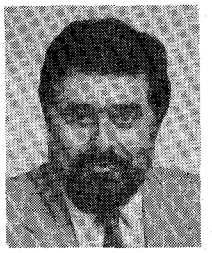

George I. Costache (M'78–SM'82) is an Associate Professor of Electrical Engineering at the University of Ottawa, Ottawa, Ont., Canada. His career has included positions with the University of Manitoba, the University of Manchester, and Electricité de France. He has taught electromagnetics and numerical techniques applied to electromagnetics for more than 18 years and has made original contributions to the solution of skin-effect problems and electromagnetic transient phenomena. His main interest is in numerical techniques, such as finite-element analysis and moment methods and their application to interference problems in steady-state and time-domain applications.

The author or coauthor of over 50 technical papers and reports, Dr. Costache is a member of the editorial review board of *COMPEL*, the international journal for computation and mathematics in electrical and electronics engineering. He is a registered Professional Engineer in the province of Ontario.

✠

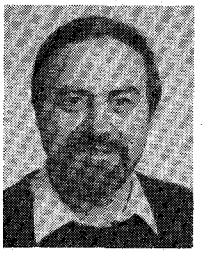

Wolfgang J. R. Hoefer (M'71–SM'78) was born in Urmitz/Rhein, Germany, on February 6, 1941. He received the diploma in electrical engineering from the Technische Hochschule Aachen, Aachen, Germany, in 1964, and the D. Ing. degree from the University of Grenoble, Grenoble, France, in 1968.

After one year of teaching and research at the Institut Universitaire de Technologie, Grenoble, France, he joined the Department of Electrical Engineering, University of Ottawa, Ottawa, Ont., Canada, where he is currently a Professor. His sabbatical activities included six months with the Space Division of the AEG-Telefunken in Backnang, Germany, six months with the Electromagnetics Laboratory of the Institut National Polytechnique de Grenoble, France, and one year with the Space Electronics Directorate of the Communications Research Centre in Ottawa, Canada. His research interests include microwave measurement techniques, millimeter-wave circuit design, and numerical techniques for solving electromagnetic problems.

Dr. Hoefer is a registered Professional Engineer in the province of Ontario, Canada.